Radar Automatic Target Recognition Based on Sequential Vanishing Component Analysis

Shengqi Liu[*], Ronghui Zhan, Jun Zhang, and Zhaowen Zhuang

Abstract—To reduce the complexity of classifier design in radar automatic target recognition (RATR), a novel RATR method for high range resolution profile (HRRP) is proposed. Linearly separable features are extracted with sequential vanishing component analysis (SVCA) which is implemented by finding the generators of each approximately vanishing polynomial set, and target classification is implemented with linear classifiers. Experiments are carried out on simulated vehicle target data and MSTAR database, and the results demonstrate the efficiency of the proposed method.

1. INTRODUCTION

The efficiency of weapon system directly depends on the target recognition capability of radar system in modern battlefield environment. A great number of literatures focused on RATR are based on radar images, such as one dimension HRRPs, synthetic aperture radar (SAR) images and inverse synthetic aperture radar (ISAR) images. A HRRP is the amplitude of the coherent summations of complex time returns from target scatterers in each range cell, which contains the target structure signatures for RATR. For the advantages in system realization, image stability and computational efficiency, HRRP-based RATR has received intensive attention from the RATR community [1–13].

In HRRP-based RATR, one primary task is how to deal with the target-aspect, time-shift, and amplitude-scale sensitivity of HRRP, which makes HRRP-based RATR a challenging problem [1, 2]. The common approaches to handle these sensitivities include [3]: dividing the training data into target-aspect frames according to some criterions to deal with the target-aspect sensitivity; amplitude-scale sensitivity is eliminated by amplitude normalization; time-shift compensation, or some time-shift invariant features are applied to remove the time-shift sensitivity. The desirable features for HRRP-based RATR should contain such characteristics: (1) stable with aspect variation, (2) invariant with time-shift, (3) separable between different classes, (4) moderate dimensionality. Most of the feature extraction methods are proposed for such purposes, and some widely investigated features are scattering center [4–6], central moment [7], high order spectrum [8], time-frequency property [9], principle component analysis [10], singular value decomposition [11], wavelet transform [12], and structure signatures of HRRPs [13], etc. A common drawback of such methods is that the spatial distribution of the extracted features is complex and unpredictable, which makes feature-based classifier design still a tough problem.

Recently, a feature extraction method referred to as vanishing component analysis (VCA) is introduced in [14]. Feature extraction is performed with the generators of approximately vanishing polynomial set, and the obtained features have the desirable property of linear separability. However, the dimension of VCA feature is proportional to the number of targets, which may result in unfeasibility for HRRP-based RATR. Motivated by such an issue, a novel recognition method based on SVCA is proposed. The generator sets found with VCA algorithm are used for feature extraction sequentially, which makes the dimension of the extracted feature approximately unchanged with the number of targets. The obtained features are proved to be linearly separable. Target classification is implemented

with linear SVM classifies. Experiments are carried out based on simulated data of 4 ground vehicle targets and MSTAR (Moving and Stationary Target Acquisition and Recognition) database. The experimental results show that the proposed method has comparable performances with VCA-based method, and both of them outperform the baseline MCC-TMM (Maximum Correlation Criterion-Template Matching Method). Additionally, the proposed method is implemented with the lowest feature dimension, meaning that it is more computationally efficient and suitable for HRRP-based RATR.

The remainder of this paper is organized as follows. In Section 2, the basic idea as well as the procedure of VCA algorithm is presented. Section 3 discusses the proposed method and its application to HRRP-based RATR. In Section 4, experiments with simulated data and real data are carried out to evaluate the recognition performances of the proposed method. Finally, conclusions are made in Section 5.

2. STATEMENT OF VCA ALGORITHM

One succinct approach to describe a point set $\mathbf{S}$ is to find a set of functions $\{f\}$ that satisfy $f(\mathbf{x}) = 0$ for each point $\mathbf{x}$ belonging to $\mathbf{S}$. In other words, if the set of functions $\mathbf{C} = \{f | f(\mathbf{x}) = 0, \mathbf{x} \in \mathbf{S}\}$ can be found, then $\mathbf{S}$ can be well characterized, and $f \in \mathbf{C}$ can be used for feature extraction. The basic idea behind VCA is to find the generators of the approximately vanishing function set under the constraint that the desired functions must be polynomials and use the generators for feature extraction. Before the detailed description of VCA algorithm is presented, some related definitions are shown as follows [14].

Definition 1 (Polynomial). A function $f : \mathbb{R}^n \to \mathbb{R}$ is called a polynomial if it is of the form $f(\mathbf{x}) = \sum_j \beta_j \mathbf{x}^{\boldsymbol{\alpha}^{(j)}} = \sum_j \beta_j \prod_{i=1}^n x_i^{\alpha_i^{(j)}}$, where $\beta_j \in \mathbb{R}$, $\boldsymbol{\alpha}^{(j)} = [\alpha_1^{(j)}, \ldots, \alpha_n^{(j)}]^T$, and each $\alpha_i^{(j)}$ is a non-negative integer. The degree of the polynomial is defined as $\max_j \|\boldsymbol{\alpha}^{(j)}\|_1 = \max_j \sum_{i=1}^n \alpha_i^{(j)}$.

Definition 2 (Ideal). A set of polynomials $\mathbf{I}$ is ideal if for any $f \in \mathbf{I}$, $g \in \mathbb{R}[x_1, \ldots, x_n]$, we have $f + g \in \mathbf{I}$ and $fg \in \mathbf{I}$ ($\mathbb{R}[x_1, \ldots, x_n]$ is the set of all polynomials in n variables $[x_1, \ldots, x_n]$ over the reals of finite degree).

Definition 3 (Set of Generators). A subset $\mathbf{F} = \{f_1, \ldots, f_k\}$ of an ideal $\mathbf{I}$ is said to generate $\mathbf{I}$, if $\forall f \in \mathbf{I}$ and there exist $g_1, \ldots, g_k \in \mathbb{R}[x_1, \ldots, x_n]$ such that $f = \sum_i g_i f_i$.

Definition 4 (Vanishing Ideal). Given a set $\mathbf{S} \subset \mathbb{R}^n$, the vanishing ideal of $\mathbf{S}$ is the set of polynomials that $\mathbf{I}(\mathbf{S}) = \{f | f(\mathbf{x}) = 0, \mathbf{x} \in \mathbf{S}\}$.

Definition 5 (Algebraic Set). A set $\mathbf{U} \in \mathbb{R}^n$ is called an algebraic set if there is a finite set of polynomials $\{p_i\}_{i=1}^k$, such that $\mathbf{U}$ are the common roots of $\{p_i\}_{i=1}^k$.

Given a point set $\mathbf{S}_m = \{\mathbf{x}^{(i)}\}_{i=1}^m (\mathbf{x} = [x_1, \ldots, x_n]^T \in \mathbb{R}^n)$, the VCA algorithm for finding a generator set for $\mathbf{I}(\mathbf{S}_m)$ is described in Algorithm 1. Since real world data are noisy, and the polynomials may "almost" vanish in the point set, VCA allows some tolerance by looking for the generator set $\mathbf{V}$ of $\mathbf{I}(\mathbf{S}_m) = \{f | f(\mathbf{x}) \leq \varepsilon, \mathbf{x} \in \mathbf{S}_m\}$. For any $\mathbf{x} \in \mathbf{S}_m$ and $\nu \in \mathbf{V}$, we have $\nu(\mathbf{x}) \leq \varepsilon$. The generator set $\mathbf{V}$ and non-vanishing polynomial set $\mathbf{F}$ are calculated iteratively, which makes an exponential increase of computational cost with the degree of polynomial avoidable in VCA algorithm.

The generator sets $\mathbf{V}_k = \{\nu_1^{(k)}, \ldots, \nu_{nk}^{(k)}\}$, $k = 1, \ldots, K$ are obtained with the VCA algorithm calculated on each point set $\mathbf{S}_k = \{\mathbf{x}_i^{(k)}, i = 1, \ldots, N_k\}$, $k = 1, \ldots, K$. All of the generators are used to define the VCA transform

$$\mathbf{x} \mapsto f_{VCA}(\mathbf{x}) = [|\mathbf{V}_1(\mathbf{x})|, \ldots, |\mathbf{V}_K(\mathbf{x})|] = \left[\left|\nu_1^{(1)}(\mathbf{x})\right|, \ldots, \left|\nu_{nK}^{(K)}(\mathbf{x})\right|\right] \tag{1}$$

The linear separability of the features after VCA transform has been proven in [14] if the intersection of any two different sets is empty, thereby good performance can be achieved with easily implemented linear classifiers.

ALGORITHM 1: VCA algorithm

1: Input: observation set $\mathbf{S}_m = \{\mathbf{x}^{(i)}\}_{i=1}^m (\mathbf{x}^{(i)} = [x_1, \ldots, x_n]^T \in \mathbb{R}^n)$, tolerance ε;
2: Output: generator set $\mathbf{V}$ and non-vanishing set $\mathbf{F}$;
3: Initialization: $\mathbf{F} = \{f(\cdot) = 1/\sqrt{m}\}$, $\mathbf{V} = \emptyset$; $\mathbf{C}_1 = \{f_1, \ldots, f_n\}$, where $f_i(\mathbf{x}) = x_i$;

Perform $(\mathbf{F}_1, \mathbf{V}_1) = \text{FindRangeNull}(\mathbf{F}, \mathbf{C}_1, \mathbf{S}_m, \varepsilon)$, $\mathbf{F} = \mathbf{F} \cup \mathbf{F}_1$, $\mathbf{V} = \mathbf{V} \cup \mathbf{V}_1$, $t = 2$;

4: Calculate: $\mathbf{C}_t = \{gh : g \in \mathbf{F}_{t-1}, h \in \mathbf{F}_1\}$;

5: If $\mathbf{C}_t \neq \emptyset$, calculate $(\mathbf{F}_t, \mathbf{V}_t) = \text{FindRangeNull}(\mathbf{F}, \mathbf{C}_t, \mathbf{S}_m, \varepsilon)$, $\mathbf{F} = \mathbf{F} \cup \mathbf{F}_t$, $\mathbf{V} = \mathbf{V} \cup \mathbf{V}_t$,

let $t = t + 1$, turn to step 4;

Otherwise, break, output $\mathbf{V}$ and $\mathbf{F}$;

ALGORITHM 2: FindRangeNull sub-procedure

1: Input: $\mathbf{F}$, $\mathbf{C}$, $\mathbf{S}_m$, ε; denote $k = |\mathbf{C}|$, $\mathbf{C} = \{f_1, \ldots, f_k\}$;

2: Calculate $\tilde{f}_i = f_i - \sum_{g \in \mathbf{F}} \langle f_i(\mathbf{S}_m), g(\mathbf{S}_m) \rangle g$, $i = 1, \ldots, k$;

3: Let $\mathbf{A} = \left[\tilde{f}_1(\mathbf{S}_m), \ldots, \tilde{f}_k(\mathbf{S}_m) \right]$, perform singular value decomposition $\mathbf{A} = \mathbf{LDU}^T$;

4: Perform $g_i = \sum_{j=1}^{k} \mathbf{U}_{j,i} \tilde{f}_j$, $i = 1, \ldots, k$;

5: Output: $\mathbf{F}_1 = \{g_i / \|g_i(\mathbf{S}_m)\| : \mathbf{D}_{i,j} > \varepsilon\}$, $\mathbf{V}_1 = \{g_i : \mathbf{D}_{i,j} \leq \varepsilon\}$.

3. RADAR TARGET RECOGNITION BASED ON SVCA

To deal with the target-aspect sensitivity of HRRP, a large number of templates must be stored as library data in training phase, and searching procedure is executed along the aspect axis for an optimal matching in test phase. In addition, the high-dimensional HRRPs may result in computational sensitivity for target classification. Thus, how to reduce the computational complexity and achieve good performance are two most important tasks for HRRP-based RATR. As can be seen from (1), the dimension of the VCA feature increases proportionally with the number of targets. For the reason the direct use of VCA feature may be unfeasible for HRRP-based RATR as a result of the highly computational complexity. Motivated by such issues, a modified method referred to as SVCA is proposed for feature extraction, and linear classifiers are used for target classification. Instead of extracting the features with all the generators of K classes, SVCA feature is calculated with each generator set separately

$$\mathbf{x} \mapsto |\mathbf{V}_k(\mathbf{x})| = \left[\left| \nu_1^{(k)}(\mathbf{x}) \right|, \ldots, \left| \nu_{nk}^{(k)}(\mathbf{x}) \right| \right] \tag{2}$$

As can be seen from (2), the feature dimension after SVCA transform is independent from the number of targets. Under the assumption that the size of each generator set is the same, the dimension of SVCA feature is compressed into $1/K$ compared to VCA feature, which makes calculation in high-dimensional feature space avoidable. Moreover, as proven in the appendix, the SVCA feature is not only separable, but also linearly separable.

Different from the VCA feature sets which are linearly separable between any two sets, the SVCA feature set calculated on the kth class is linearly separable with the rest of $K-1$ classes, while the linear separability among $K-1$ classes is not referred. However, comparable performance can be obtained with linear classifiers as shown in Section 4. The matrixes for feature transformation and the optimal weights of linear classifiers are acquired with (2) and linear support vector machine (SVM) [15], respectively. Both of them can be calculated offline.

It has been reported that the target-aspect sensitivity can be mitigated effectively by averaging the HRRPs over a large aspect angle [1]. For the reason incoherent average is calculated firstly in a subset of HRRPs from a target-aspect sector without scatterers' motion through range cells [2], then feature extraction is performed with SVCA. No less than $K - 1$ binary-classification classifiers are needed for the classification of K targets, which can be organized as serial mode or parallel mode. Classification is carried out sequentially in serial mode, and binary decision is made for each test sample. At iteration k, if "1" denotes the output of the kth classifier, then the test sample is labeled with k, and iteration is terminated. Otherwise, iteration is repeated for $k = k + 1$. In parallel mode, the test sample is imported into all the linear classifiers simultaneously, and binary decision is made for each classifier as well. Obviously, parallel implementation mode is much more computationally efficient, so it is selected for real-time RATR in this paper.

Based on the above analysis, the proposed method can be summarized as follows:

Training Phase: Let $\mathbf{S} = \{\mathbf{x}_i^{(k)}\}$, $i = 1, \ldots, N_k$, $k = 1, \ldots, K$ be a set of labeled training samples which contains K classes, where N_k denotes the number of samples of each class. At iteration k, $\mathbf{S}$ is divided into two subsets $\mathbf{S}_A$ and $\mathbf{S}_B$, where $\mathbf{S}_A = \mathbf{S}_k$, $\mathbf{S}_B = \cup_{l=1, l \neq k}^{K} \mathbf{S}_l$. The transformation matrix is obtained with SVCA based on $\mathbf{S}_A$, and linearly separable feature sets $\mathbf{F}_A$ and $\mathbf{F}_B$ can be acquired through feature extraction performed on $\mathbf{S}_A$ and $\mathbf{S}_B$. Next, the training of linear SVM classifier is carried out based on $\mathbf{F}_A$ and $\mathbf{F}_B$. The iteration is repeated until the training of K linear classifiers is accomplished, and then the classifiers are organized with parallel mode.

Test Phase: The test sample $\mathbf{x}$ is imported into K linear classifiers simultaneously, and binary decision is made in each classifier. Generally there is only a "1" output which indicates the test sample label. Otherwise, $\mathbf{x}$ is assigned to the label which has the largest distance to the corresponding decision hyperplane.

4. EXPERIMENTAL RESULTS AND ANALYSIS

4.1. Toy Example

We begin with a toy example to evaluate the feasibility of the VCA/SVCA features used for target classification. The two classes are shaped as circles in two dimension plane, corresponding to the equations $\mathbf{X} = \{\mathbf{x}|x_1^2 + x_2^2 = 1\}$ and $\mathbf{Y} = \{\mathbf{y}|y_1^2 + y_2^2 = 9\}$. The observations are generated with uniform sampling on the circles and adding with uniform random numbers. The spatial distributions of the raw data and SVCA features are shown in Figure 1. As can be seen clearly, the two classes are nonlinearly separable in raw data space, while linearly separable in SVCA feature space, meaning that nonlinearly separable data are turned linearly separable after SVCA transform. Thus, we can use linear classifiers to achieve good classification results.

In the following experiments, odd samples are used for training and even for testing. Classification experiments with linear SVM classifiers are carried out based on raw data, VCA and SVCA features. Table 1 lists the correct classification rates (CCRs) of the three methods averaged by 100 Monte-Carlo trials. It can be seen from the performance comparison that significant improvement appears using VCA/SVCA features, demonstrating that target classification based on VCA/SVCA features is feasible.
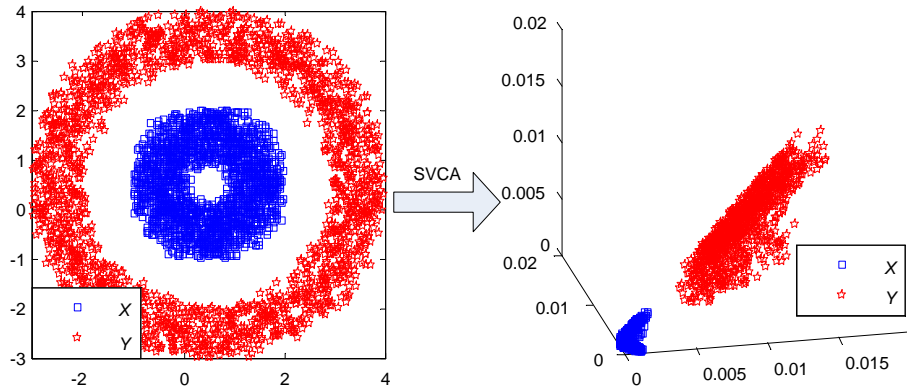

Figure 1. Spatial distributions of raw data and SVCA features.

Table 1. Correct classification rates of toy example.

	X	Y
Raw data	88.9%	39.47%
VCA feature	100%	99.99%
SVCA feature	100%	99.88%

4.2. Experiments with Simulated Database

In this subsection we turn to examine the proposed method based on simulated database. A database of range profiles for four ground vehicle targets including an armored carrier, heavy carrier, heavy-duty truck and wagon truck is developed. The detailed parameters for radar cross-section generation are shown in Table 2. The CAD model of each vehicle (as shown in Figure 2) is exported as a facet file for electromagnetic simulation software, which generates the radar echoes from 0 to 60 deg aspect in 0.1 deg increments, resulting in 601 profiles. The range profiles are formed through inverse fast Fourier transform (IFFT), with each consisting of 128 range cells. HRRPs illuminated at depression angle 27 deg are used for training, and 30 deg are used for testing. Figure 2 shows the HRRPs observed at depression angle 27 deg and aspect angle 50 deg as examples. The amplitude-scale sensitivity of HRRP is eliminated by amplitude normalization (L_2 normalization) while time-shift compensation is unnecessary for the turntable-like HRRP data. The incoherent average of the training range profiles subtending a 3 deg aspect aperture is exported for VCA/SVCA feature extraction in training phase, and single-view range profiles are imported for testing directly in test phase.

Table 2. Electromagnetic simulation software settings.

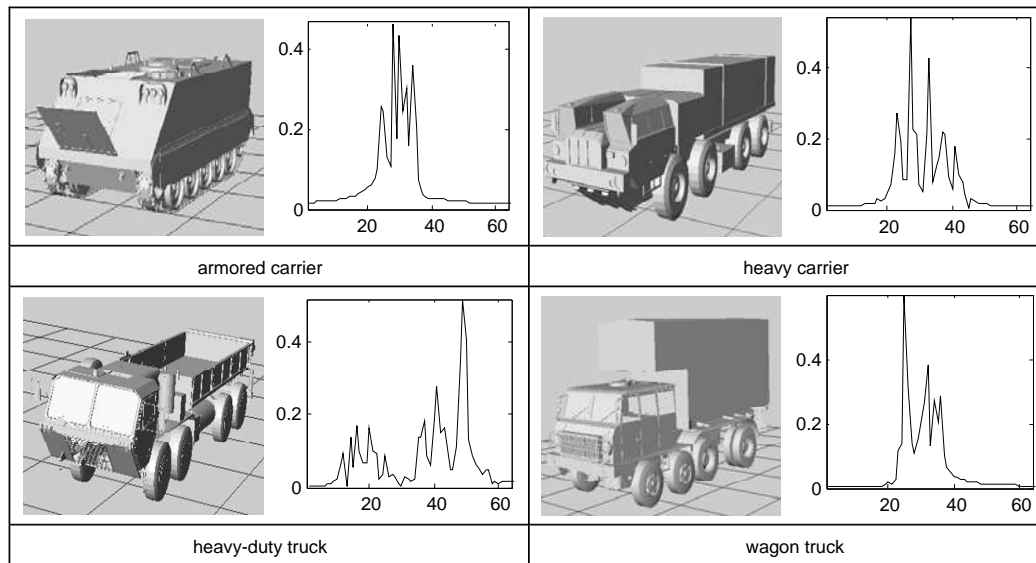| Center frequency	10 GHz	Azimuth angles	0∼60 deg in 0.1 deg steps
Bandwidth	500 MHz	Depression angles	27 deg, 30 deg
Number of frequency samples	128	Polarization mode	HH

Figure 2. Simulated vehicle targets and HRRPs. Horizontal axis indicates the range bins, and vertical axis represents the normalized amplitude.

We compare the classification performance of the proposed method with the baseline MCC-TMM and summarize the results in the form of confusion matrix as shown in Table 3. Across each row of the confusion matrix, the numbers represent the occurrences of the test samples from a particular test target type (indicated in the head of the row) which are classified as the target types indicated on the top of each column. In Table 3, the numbers outside the parentheses are the classification results performed with SVCA-based method, and those in the parentheses represent the numbers of test samples classified with MCC-TMM. It can be seen that the average CCR is improved from 90.97% to 93.88%. Additionally, the dimensions of the SVCA features for the four vehicle targets are 32, 42,

Table 3. Comparison of SVCA-based method and MCC-TMM on simulated database.

	armored carrier	heavy carrier	heavy-duty truck	wagon truck	Correct rate (%)
armored carrier	562 (523)	9 (17)	12 (5)	18 (56)	93.51 (87.02)
heavy carrier	18 (5)	575 (586)	3 (2)	5 (8)	95.67 (97.50)
heavy-duty truck	3 (23)	5 (8)	592 (554)	1 (16)	98.50 (92.18)
wagon truck	54 (26)	14 (38)	5 (13)	528 (524)	87.85 (87.19)
Average correct classification rate: SVCA — 93.88%, MCC-TMM — 90.97%					
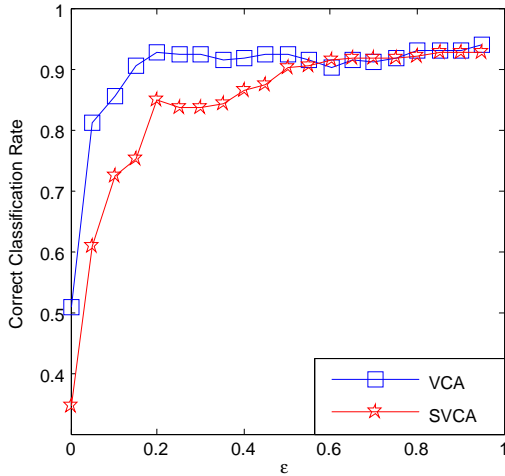
Figure 3. Correct classification rates under different ε.
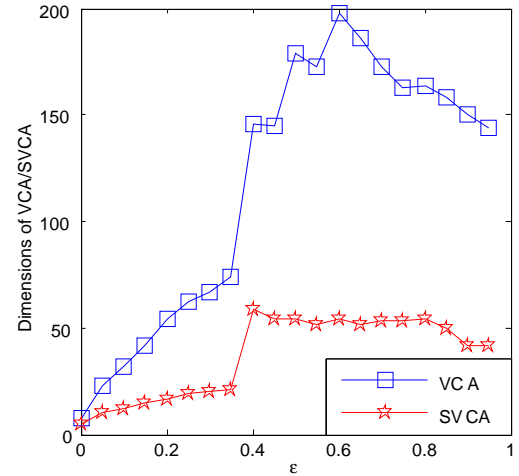
Figure 4. Feature dimensions with different ε.

54, and 36, respectively, which are much lower than the raw HRRPs (128). Moreover, the searching procedure for an optimal matching along aspect axis is avoidable, which makes the proposed method much more efficient for target classification.

In the following paragraph the effect of the parameter will be discussed. Both the linear separability and the dimensions of the extracted features are changed with the tolerance ε. The average CCRs under different ε are shown in Figure 3. It can be seen from the figure that both the performance of VCA-based and SVCA-based method improve with the increase of ε for $\varepsilon < 0.5$, and they are nearly constant for $\varepsilon > 0.6$. As mentioned previously, ε stands for the tolerance to noise and the mismatch of the polynomial model. This means that a larger ε has more tolerance capability and is more beneficial to performance improvement. It is also seen from the performance comparison between SVCA-based and VCA-based method that the CCRs are comparable for $\varepsilon > 0.6$, which indicates that the separability of SVCA features is nearly the same as VCA features. Moreover, much lower dimensional features are used in SVCA-based method (as shown in Figure 4, the SVCA feature dimension is the maximum for the four targets), which will significantly reduce the computational burden for target classification.

In an attempt to analyze the effect of observation noise on target classification, different signal-to-noise ratio (SNR) is considered for performance evaluation. The SNR is defined as [16]:

$$\text{SNR (dB)} = 10 \log_{10} \left(\frac{\sum_{l=1}^{L} p_l}{L \cdot \sigma^2} \right) \tag{3}$$

where p_l denotes the power of the original test HRRP in the lth range cell, σ^2 the power of Gaussian white noise, and L the number of range cells which can be estimated by taking the difference between the first bin and last bin to cross the threshold along the range profile. The threshold is defined as the amplitude-ratio to the peak of range profile, which is set to 0.1 in our experiments.
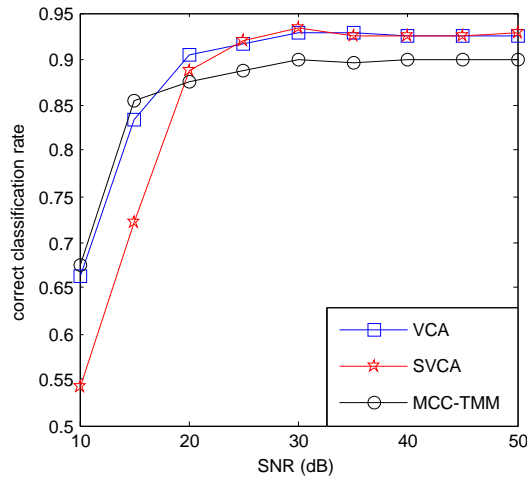
Figure 5. Classification performance with SNR via VCA, SVCA and MCC-TMM.

Figure 5 shows the average CCRs for 100 Monte-Carlo trials under different SNRs, obtained via MCC-TMM, VCA-based and SVCA-based method. As can be seen from the figure, the performance of SVCA-based method is a little worse than MCC-TMM and VCA-based method under low-SNR cases. It can be explained as that noise and the mismatch of the polynomial model in low-SNR cases are beyond the tolerance capability. It is also noted that SVCA- and VCA-based methods have comparable performance and outperform MCC-TMM with the increase of SNR (SNR > 20 dB). Furthermore, SVCA-based method has lower dimensional features for target classification than MCC-TMM and VCA-based method. All the above can be concluded as that the proposed method has superior performance and higher efficiency for HRRP-based RATR.

4.3. Experiments with MSTAR Database

In this subsection we evaluate the performance of the proposed method using the MSTAR public database. The MSATR database contains X-band SAR images captured at depression angles 15 deg and 17 deg over the full aspect angles with $1 \, \text{ft} \times 1 \, \text{ft}$ resolution for 10 ground vehicle targets. A detailed description about MSATR database is given in [17]. HRRPs are extracted from SAR images, and the creation process is illustrated in Figure 6 [18].
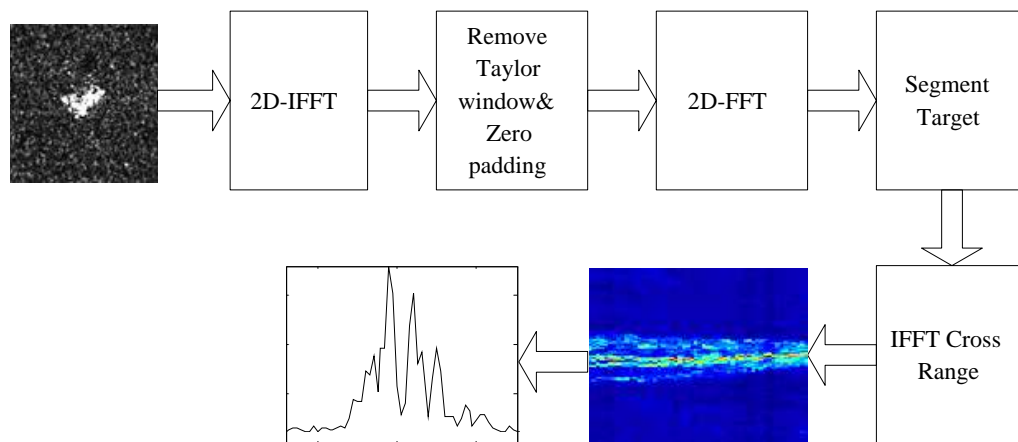

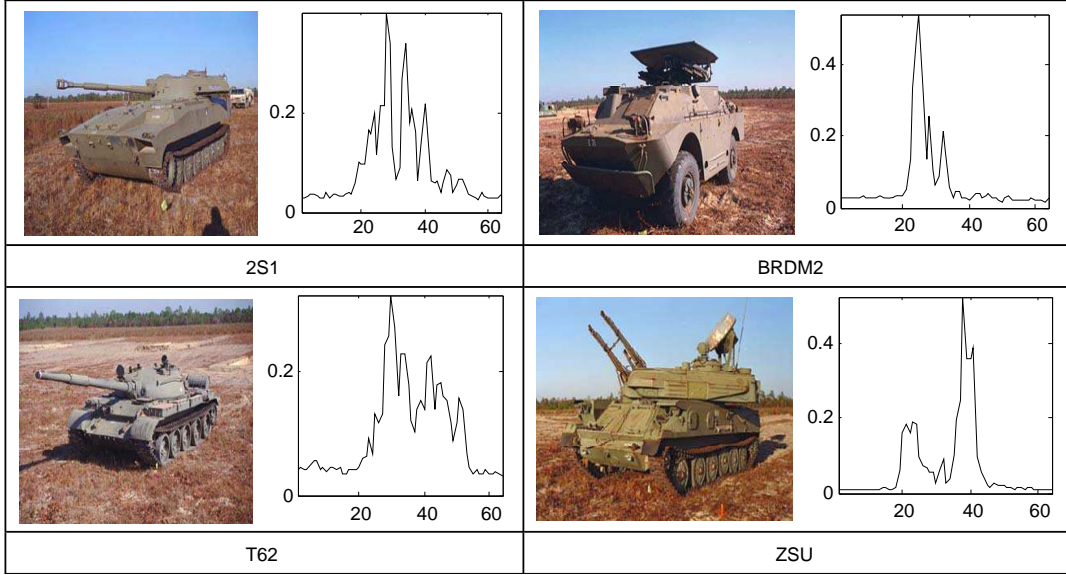**Figure 6.** The HRRP creation process from SAR images.

Figure 7. MSTAR targets and HRRPs extracted from SAR images. Horizontal axis indicates the range bins, and vertical axis represents the normalized amplitude.

Table 4. Classification results on the MSTAR database with SVCA-based method.

	2S1	BRDM2	T62	ZSU4
2S1	251	6	14	3
BRDM2	6	262	3	3
T62	15	0	244	14
ZSU4	1	0	8	265
Average correct classification rate: 93.17%				

Table 5. Classification results on the MSTAR database with MCC-TMM.

	2S1	BRDM2	T62	ZSU4
2S1	237	12	11	14
BRDM2	15	258	1	0
T62	8	1	239	25
ZSU4	1	0	21	252
Average correct classification rate: 89.62%				

Table 6. Runtimes of 3 methods.

	MCC-TMM	VCA	SVCA
Runtime (s)	43.11	4.74	2.18

In the following experiments, data measured at depression angle 17 deg are used as library data, and 15 deg is considered as unknown input for testing. Specifically, four vehicle targets (2S1, RDM2, 62 and ZSU) which cover most completed aspect angles are selected for performance evaluation (as shown in Figure 7). One average HRRP is extracted from each SAR image. In training phase, the HRRP dataset over full 360 deg aspect angles is divided into 6 subsets, with each covering a 60 deg azimuth aperture. In test phase, classification of each test sample is carried out in the actual angle subset by assuming that aspect angle prediction through SAR image provides approximate target-heading information. The classification results of SVCA-based method and MCC-TMM are summarized in Table 4 and Table 5 with the same processing procedure described in the previous subsection, and both of them are represented in the form of confusion matrix. As can be seen from the tables, SVCA-based method outperforms MCC-TMM on the MSTAR database. In conclusion, the experimental results also verify the superior performance of the proposed method.

The computational efficiency of the proposed method can be seen by comparing the runtimes of MCC-TMM, VCA-based and SVCA-based methods. The three methods are executed under the same

PC environment with 2.8 GHz CPU, 2.75 GB RAM, MATLAB (R2011a) simulation software. After the acquisition of the optimal parameter ε and the weighted vectors for linear classifiers offline in training phase, HRRPs extracted from SAR images are filled into each classifier for testing. The time consumptions of MCC-TMM, VCA-based and SVCA-based methods for 1095 test samples are shown in Table 6. It is clearly seen that the SVCA-based method consumes the least time, which demonstrates the high efficiency of the proposed method.

5. CONCLUSION

Due to the complex distribution of the features extracted with conventional methods, classifier design based on the features is still a challenging problem. Aiming at the issue, a novel recognition method is proposed for HRRP-based RATR. Linearly separable features are extracted with SVCA, and target classification is implemented with linear SVM classifiers. Experimental results carried out on simulated and real data demonstrate that the proposed method outperforms the baseline MCC-TMM, has comparable performance with VCA-based method and is much more computationally efficient, indicating its potential use for real-time RATR applications.

ACKNOWLEDGMENT

APPENDIX A.

The proof of the linear separability for SVCA features.

A.1. Proof of Separability

Assume that there are algebraic sets $\{\mathbf{U}_k\}_{k=1}^K$ whose intersection is empty in pairs such that $\mathbf{S}_k \subseteq \mathbf{U}_k$, and let $\mathbf{V}_k = \{\nu_1^{(k)}, \ldots, \nu_{nk}^{(k)}\}$ denote the generator set of $\mathbf{I}(\mathbf{U}_k)$, then we have $\mathbf{V}_k \in \mathbf{I}(\mathbf{U}_k)$. For each $\mathbf{x} \in \mathbf{U}_k$, $\nu_i^{(k)} \in \mathbf{V}_k$, we have $|\nu_i^{(k)}(\mathbf{x})| < \varepsilon$. From the definition of vanishing ideal, it is obvious that $\mathbf{x}$ is a common root of $\mathbf{I}(\mathbf{U}_k)$. Suppose that there are some $\mathbf{x}' \in \mathbf{U}_l$ vanishing on $\mathbf{V}_k$, for some $l \neq k$. That means $|\nu_i^{(k)}(\mathbf{x}')| < \varepsilon$, for all i. Therefore, $\mathbf{x}'$ is a common root of $\mathbf{V}_k$. It follows immediately that $\mathbf{x}'$ is also a common root of $\mathbf{I}(\mathbf{U}_k)$, thus $\mathbf{x}' \in \mathbf{U}_k$, which contradicts the assumption that $\mathbf{U}_l \cap \mathbf{U}_k = \emptyset$. In other words, for each $\mathbf{x}' \in \mathbf{S}_l(l \neq k)$, there must be some i such that $|\nu_i^{(k)}(\mathbf{x}')| > \varepsilon$. On the contrary, for any $\mathbf{x} \in \mathbf{S}_k$, the inequation $|\nu_i^{(k)}(\mathbf{x})| < \varepsilon$ holds for all i. This means SVCA features are separable.

A.2. Proof of Linear Separability

Suppose that $\mathbf{F}^k = \{\boldsymbol{\alpha}_i\}_{i=1}^N$ and $\mathbf{F}^l = \{\boldsymbol{\beta}_i\}_{i=1}^N$ are the SVCA feature sets calculated on $\mathbf{S}_k$ and $\mathbf{S}_l(l \neq k)$ with the generator set $\mathbf{V}_k$, respectively. Without loss of generality, if there are some $\boldsymbol{\omega} = [\omega_1, \ldots, \omega_n]^T$ which satisfy $\boldsymbol{\omega}^T\boldsymbol{\alpha} - \boldsymbol{\omega}^T\boldsymbol{\beta} < 0$ for any $\boldsymbol{\alpha} \in \mathbf{F}^k$ and $\boldsymbol{\beta} \in \mathbf{F}^l$, then $\mathbf{F}^k$ and $\mathbf{F}^l$ are linearly separable. Denote $\boldsymbol{\alpha}_k = [\alpha_1, \ldots, \alpha_n] = \arg\max_{\boldsymbol{\alpha}} \boldsymbol{\omega}^T\boldsymbol{\alpha}$ and $\boldsymbol{\beta}_l = [\beta_1, \ldots, \beta_n] = \arg\min_{\boldsymbol{\beta}} \boldsymbol{\omega}^T\boldsymbol{\beta}$, then we have $\alpha_i < \varepsilon$ for each i and $\beta_i > \varepsilon$ for some i. Clearly, let $\omega_i < 0$ if $\varepsilon - \beta_i > 0$ and $\omega_i > 0$ if $\varepsilon - \beta_i < 0$, then $\boldsymbol{\omega}^T\boldsymbol{\alpha} - \boldsymbol{\omega}^T\boldsymbol{\beta} < 0$ holds for any $\boldsymbol{\alpha} \in \mathbf{F}^k$ and $\boldsymbol{\beta} \in \mathbf{F}^l$, which concludes that $\mathbf{F}^k$ and $\mathbf{F}^l$ are linearly separable.

REFERENCES

1. Xing, M., Z. Bao, and B. Pei, "Properties of high-resolution range profiles," *Optical Engineering*, Vol. 41, No. 2, 493–504, 2002.

2. Du, L., H. Liu, Z. Bao, et al., "A two-distribution compounded statistical model for radar HRRP target recognition," *IEEE Transactions on Signal Processing*, Vol. 54, No. 6, 2226–2238, 2006.

3. Du, L., "Study on radar HRRP target recognition," Xidian University, Xi'an, China, 2007.

4. Liao, X. J., P. Runkle, and L. Carin, "Identification of ground targets from sequential high-range-resolution radar signatures," *IEEE Transactions on Aerospace and Electronic Systems*, Vol. 38, No. 4, 1230–1242, 2002.

5. Fu, Y. W., Y. P. Jia, and Z. W. Zhuang, "Radar target classification based on one dimensional scattering centers matching," *Acta Electronica Sinica*, Vol. 34, No. 3, 404–408, 2006.

6. Yan, X. W., J. M. Hu, G. Zhao, J. Zhang, and J. Wan, "A new parameters estimation method for GTD model based on modified compressed sensing," *Progress In Electromagnetics Research*, Vol. 141, 553–575, 2013.

7. Fan, P. and Z. R. Jing, "Research on one-dimensional scattering center feature extraction from radar targets," *Systems Engineering and Electronics*, Vol. 30, No. 12, 2352–2354, 2008.

8. Du, L., H. W. Liu, et al., "Radar HRRP target recognition based on higher order spectra," *IEEE Transactions on Signal Processing*, Vol. 53, No. 7, 2359–2368, 2005.

9. Pan, M., D. Lan, et al., "Multi-task hidden Markov modeling of spectrogram feature from radar high-resolution range profiles," *EURASIP Journal on Advances in Signal Processing*, Vol. 86, No. 1, 1–17, 2012.

10. Prasad, S. and L. M. Bruce, "Decision fusion with confidence-based weight assignment for hyperspectral target recognition," *IEEE Transactions on Geoscience and Remote Sensing*, Vol. 46, No. 5, 1448–1458, 2008.

11. Arnab, K. S., S. P. Anindya, and W. Robert, "Eigen-template-based HRR-ATR with multi-look and time-recursion," *IEEE Transactions on Aerospace and Electronic Systems*, Vol. 49, No. 4, 2396–2385, 2013.

12. Pass, M. M. D., "Wavelet feature extraction of high-range resolution radar profiles using generalized Gaussian distributions for automatic target recognition," Claremont Graduate University, California, USA, 2006.

13. Pilcher, C. M. and K. Alireza, "Paritime ATR using classifier combination and high resolution range profiles," *IEEE Transactions on Aerospace and Electronic Systems*, Vol. 47, No. 4, 2558–2573, 2011.

14. Roi, L., L. David, et al., "Vanishing component analysis," *The 30th International Conference on Machine Learning*, Vol. 28, No. 1, 597–605, Atlanta, USA, 2013.

15. Sun, J. X., *Modern Pattern Recognition,* 2nd Edition, Higher Education Press, Beijing, China, 2008.

16. Pan, M., L. Du, et al., "Noise-robust modification method for Gaussian-based models with application to radar HRRP recognition," *IEEE Geoscience and Remote Sensing Letters*, Vol. 10, No. 3, 558–562, 2013.

17. Mossing, J. C. and T. D. Ross, "An evaluation of SAR ATR algorithm performance sensitivity to MSTAR extended operating conditions," *Proceeding of SPIE, Algorithm for Synthetic Aperture Radar Imagery V*, E. G. Zelnio (ed.), Vol. 3370, 554–565, 1998.

18. David, G., O. Michael, et al., "Preliminary comparison of high range resolution signature of moving and stationary ground vehicles," *Proceeding of SPIE*, Vol. 4727, 2002.